ACS OMEGA

http://pubs.acs.org/journal/acsodf

Article

Coupled Typical Coke Gasification and Sintering Ore Reduction in $CO-N_2-H_2$

Jinglan Hu, Yuelin Qin,* Xin Li, Haowen Liu, Yin Deng, and Hao Liu

Cite This: *ACS Omega* 2022, 7, 34420−34427

Read Online

ACCESS | Metrics & More | Article Recommendations

ABSTRACT: Through thermodynamic calculation and high-temperature simulation experiments, the coupling behavior between gasification of high- and low-reactivity cokes and reduction of sintering ore in $CO-N_2-H_2$ mixed gas with 25% H_2 volume fraction was studied, and the evolution of the coke carbon structure and the pore structure was analyzed. The results show that the reaction rate of the two cokes increases with the increase in temperature after the coupling reaction, and the strength after drumming decreases with the increase in temperature. The strength of low-reactivity coke after the reaction is higher than that of high-reactivity coke, and the reduction degree of sintering ore after the coupling reaction with low-reactivity coke is higher than that with high-reactivity coke. At high temperatures and high hydrogen-rich atmospheres with $\varphi(H_2)$ of 25%, the strength of high-reactivity coke after drum rotation is greater than 60.4%. The graphitization degree and carbon structure order of low-reactivity coke are higher than those of high-reactivity coke.

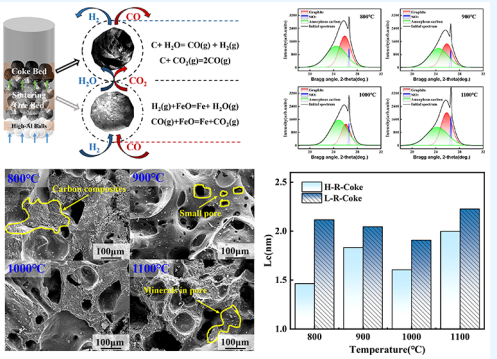

1. INTRODUCTION

In recent years, various environmental problems caused by the greenhouse effect have attracted worldwide attention. The iron and steel industry is an important basic industry in the industrialized countries of the world, and it is also an industry with high energy consumption and high pollution. Blast furnace ironmaking is the main source of molten iron in steel production and has not been replaced by other processes. The consumption of fossil fuels such as coke in a blast furnace is an important source of carbon dioxide emissions. It is very difficult to excavate the energy-saving and emission reduction potential of traditional production processes through advanced technology. Hydrogen, as a reducing agent, causes no pollution and is an ideal substitute for carbon. Therefore, some researchers have proposed a hydrogen metallurgy process represented by blast furnace hydrogen-rich smelting technology, including blast furnace injection of coke oven gas,[1−4] coal manufacturing gas, and natural gas,[5,6] or other hydrogen-containing substances.[7,8]

After the blast furnace is rich in hydrogen, the deterioration of coke in the blast furnace is mainly caused by the dissolution reaction. There are two different cases of coke dissolution reaction: one is the carbon dissolution reaction between coke and CO_2, and the other is the water-gas reaction between coke and H_2O. At present, researchers have mainly explored the effects of pure H_2O, pure CO_2, or their mixture on the dissolution behavior and performance of coke. Wang et al. found that the temperature loss of coke caused by H_2O was about 37 °C and 125 °C lower than that caused by CO_2.[9−11] The gasification rate of coke with H_2O was about 1.27−3.16 times higher than that of CO_2, and the location of the gasification reaction between coke and H_2O was closer to the outside of coke. Chang et al. studied the effects of CO_2 and H_2O on gasification dissolution and the deep reaction of coke. The results show that the average reaction rate of coke with H_2O is about 1.3−6.5 times that of CO_2 at 950−1250 °C. With the increase of pressure, the gasification dissolution reaction of coke transfers to a high-temperature zone.[12] Zhang studied the kinetics of the coke gasification reaction in CO_2-CO-N_2 with or without H_2 by thermogravimetry. When the temperature is low, the gasification rate with hydrogen is significantly higher than that without hydrogen.[13] In addition, some researchers also comparatively analyzed the effects of H_2O and CO_2 on the microstructure of coke and pointed out that the damage of H_2O on the coke structure was greater than that of CO_2, and the erosion of H_2O on the coke pore wall was more serious.[14−17] Whether the reactivity of coke is an important factor that determines the performance of blast furnaces has always been the subject of debate. Low-reactivity coke is widely used as the main reducing agent for blast furnace ironmaking in the steel industry. However, relevant theoretical research and production

Received: June 29, 2022
Accepted: September 7, 2022
Published: September 15, 2022

https://doi.org/10.1021/acsomega.2c04064
ACS Omega 2022, 7, 34420−34427

practice have demonstrated that it is feasible to use high-reactivity coke for hydrogen-rich blast furnaces.[18−22]

The above literature shows that these studies focus on the influence of pure CO_2 and pure H_2O on the coke gasification reaction and iron-bearing material reduction. In the actual production process of a blast furnace, CO_2 and H_2O produced by iron oxide reduction are the main sources of the coke gasification reaction due to the special arrangement between an iron-bearing material such as sintering ore and coke. Therefore, the dissolution loss behavior of coke in a blast furnace is closely related to the reduction of the iron-bearing material. However, there are few studies on this aspect, and the analysis of the dissolution loss behavior of coke during the coupling reaction of coke and an iron-bearing material such as sintering ore is lacking. Especially, after the blast furnace is rich in hydrogen, the H_2 content of the bosh gas can reach 14−20%, and its indirect reduction with iron ore produces a large amount of H_2O, which has a more obvious influence on coke performance.[15] Therefore, based on the hydrogen-rich smelting of the blast furnace, the coupling effects of iron oxide reduction and coke gasification under different $\varphi(H_2)$ were analyzed by thermodynamic calculation. The coupling behavior of high- and low-reactivity coke gasification and sintering ore reduction under a high hydrogen-rich atmosphere ($\varphi(H_2)$ = 25%) was studied by a high-temperature reduction experiment. It is expected that the research results can provide a reliable theoretical basis for the application of blast furnace hydrogen-rich smelting technology and high-reactivity coke.

2. THERMODYNAMIC ANALYSIS OF COUPLING REACTION

The main gas components in a hydrogen-rich BF include N_2, H_2, H_2O, CO, and CO_2. N_2 is not involved in the reaction; CO and H_2 are involved in the reduction of iron oxides to produce CO_2 and H_2O, respectively. The gasification reaction of CO_2 and H_2O with coke is an important cause of coke deterioration. Therefore, there is a coupling effect between coke gasification and sintering ore reduction in a hydrogen-rich BF. As shown in Table 1, the reduction reaction of iron oxide and the gasification reaction of coke in a BF are listed, in which the reduction reaction of Fe_2O_3 is ignored because the reaction is irreversible.

Table 1. Main Chemical Reaction Equations

chemical reaction equations		$\Delta_r G_m^\theta$
$CO(g) + 1/4Fe_3O_4 = 3/4Fe + CO_2(g)$	(1)	$-8287 + 9.993T$
$H_2(g) + 1/4Fe_3O_4 = 3/4Fe + H_2O(g)$	(2)	$29\,369 - 25.07T$
$CO(g) + FeO = Fe + CO_2(g)$	(3)	$-18\,628 + 22.17T$
$H_2(g) + FeO = Fe + H_2O(g)$	(4)	$16\,826 - 10.30T$
$CO(g) + Fe_3O_4 = 3FeO + CO_2(g)$	(5)	$26\,044 - 30.44T$
$H_2(g) + Fe_3O_4 = 3FeO + H_2O(g)$	(6)	$61\,473 - 62.88T$
$C + CO_2(g) = 2CO(g)$	(7)	$166\,500 - 171T$
$C + H_2O = CO(g) + H_2(g)$	(8)	$133\,100 - 141.63T$

The thermodynamic equilibrium diagram of the coupling reaction between iron oxide reduction and coke gasification at different H_2 volume fractions ($\varphi(H_2)$) was calculated and drawn using thermodynamic software (FactSage) under atmospheric pressure, as shown in Figure 1. In the thermodynamic calculation process, the total amount of the initial reducing gas was set to be 1 mol, and the initial atmosphere of the reaction was CO−H_2−N_2, where the volume fraction of CO was fixed at 42%. The reduction reactions of iron oxide were investigated when the volume fractions of H_2 were 0, 5, 15, and 25%. Then, according to the volume fractions of CO and H_2, the gasification reactions of CO_2 and H_2O generated after iron oxide reduction with coke in Table 1 were calculated in equal proportion.

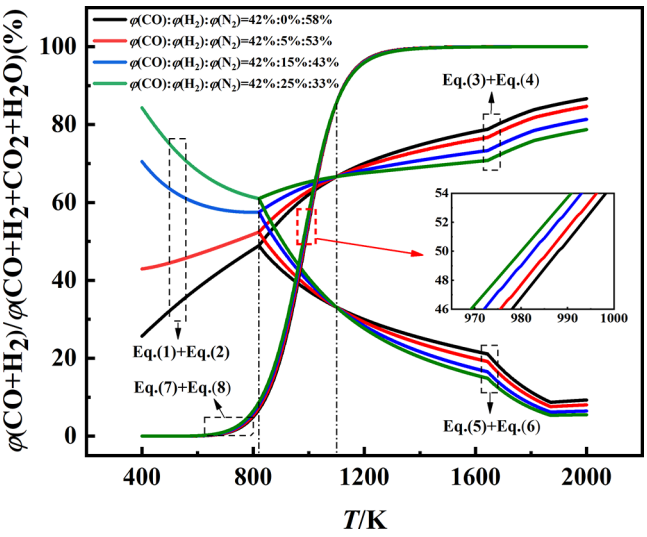

Figure 1. Thermodynamic equilibrium diagram of the coupling reaction between iron oxide reduction and coke gasification under different $\varphi(H_2)$.

In Figure 1, when the temperature is less than 1100 K, the concentration of reducing gas in the system increases when the iron oxide reduction reaction reaches equilibrium with the increase of the H_2 volume fraction ($\varphi(H_2)$) in the initial reaction gas. According to the principle of minimum free energy, it is not conducive to the further reduction of iron oxide, and the reduction reaction is mainly controlled by CO. Additionally, CO_2 and H_2O generated by the reduction of iron oxide also decreased, resulting in the inhibition of coke gasification. However, when the temperature is greater than 1100 K, the corresponding thermodynamic calculation results are reversed. This is consistent with the thermodynamic results calculated by Lan et al. under different $\varphi(CO)/\varphi(H_2)$.[23]

The preceding results demonstrate that the arrangement of iron ore and coke layers in a blast furnace causes a coupling effect between coke gasification and sintering ore reduction. In a hydrogen-rich BF, when the contents of CO and H_2 change, the contents of CO_2 and H_2O generated in the reduction process of iron ore are directly affected, thereby affecting the gasification reaction of coke. The thermodynamic method can only determine the energy relationship and the direction and limit of the change, but it does not involve the steps, rate, and process mechanism. Consequently, it is necessary to explore the coupling behavior of typical coke gasification and sintering ore reduction by simulating the atmosphere of a hydrogen-rich BF.

3. EXPERIMENTAL SECTION

3.1. Materials. The cokes used in the study are of two kinds with obvious reactivity differences, which are low-reactivity coke from Chongqing Iron and Steel Company (L-R coke) and high-reactivity coke from Xinjiang Bayi Iron and Steel Company (H-R coke). The sintering ore from Xinjiang Bayi Iron and Steel Company and its chemical composition analysis are shown in

https://doi.org/10.1021/acsomega.2c04064
ACS Omega 2022, 7, 34420−34427

Table 2. The coke reactivity index (CRI), strength after reaction (CSR), and industrial analysis results are shown in Table 3. The

Table 2. Chemical Composition of Sintering Ore (%)

TFe	Al_2O_3	CaO	MgO	SiO_2	FeO	S	P
54.7	1.01	11.1	1.7	5.97	9.52	0.046	0.093

meaning of the abbreviations used in this paper is shown in Table 4.

Table 3. Industrial Analysis, CRI, and CSR of Coke

	industrial analysis (%)					
name	M_{ad}	V_{ad}	A_d	FC_d	CRI (%)	CSR (%)
H-R coke	0.36	1.17	12.05	86.66	53.40	20.82
L-R coke	0.58	1.87	11.77	85.78	25.20	65.24

Table 4. Description of the Meaning of Abbreviations

abbreviation	implication
CRI	coke reactivity index under the GB/T4000-2008 standard test method
CSR	strength index of coke after reaction under the GB/T4000-2008 standard test method
CRE	reaction rate of coke after the coupling reaction of coke gasification and sintering ore reduction
CTS	strength of coke after drum rotation after the coupling reaction of coke gasification and sintering ore reduction
RI_t	reduction degree of sinter after the coupling reaction of coke gasification and sintering ore reduction

3.2. Experimental Apparatus. The schematic diagram of the device for the coupling reaction experiment is shown in Figure 2, which is mainly composed of a reaction furnace, gas

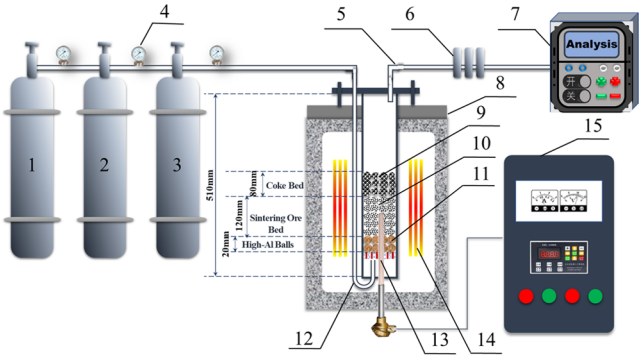

Figure 2. Schematic diagram of the experimental apparatus for the coupling reaction. 1, CO; 2, H_2; 3, N_2; 4, mass flowmeter; 5, gas outlet; 6, gas purification device; 7, gas analyzer; 8, water-cooled cover; 9, coke; 10, sintering ore; 11, high-Al ball; 12, gas inlet; 13, thermocouple; 14, heater; and 15, furnace controller.

distribution system, control system, and flue gas analysis system. The reaction tube is a $\Phi 80 \times 5 \times 800$ mm^3 fused corundum tube.

3.3. Experimental Methods. The sintering ore and coke were ground to 23−25 mm diameter and dried at 378 ± 5 K for 2 h. The ratio of sintering ore to coke was 4:1, that is, 200 ± 0.5 g coke and 800 ± 0.5 g sintering ore. The sintering ore and coke were charged into the reaction tube with the furnace heating up. Coke was in the upper layer, sintering ore was in the lower layer, and the heating rate was 10 K/min. When the temperature rose to 400 °C, the protective gas N_2 (2 L/min) was introduced. N_2 was stopped when the temperature reached the experimental predetermined temperature (800−1100 °C). At the predetermined temperature, the reaction gas ($CO/N_2/H_2$ = 42%:33%:25%) was injected at a flow rate of 5 L/min, and the purity of the gas was 99.99%. After a constant temperature reaction for 4 h, the heating was stopped and N_2 (2 L/min) was introduced into the cooling process. The content of each component in the mixture was controlled by adjusting the gas flow rate during the experiment. When the temperature of the reaction tube was lower than room temperature (25 °C), the coke and sintering ore were taken out and weighed, separately, and then, the thermal strength of the coke was measured. All of the coke after the reaction was charged into the I-type drum and rotated at a speed of 20 rpm/min for 600 rpm. The coke was taken out for screening and weighed with a 10 mm round hole. The CTS of coke and CRE of coke after the reaction were calculated by formulas 9 and 10, respectively. In addition, the RI of sintering ore after the coupling reaction was calculated by formula 11 as follows

$$\mathrm{CRE} = \frac{m_0 - m_1}{m_0} \times 100\% \tag{9}$$

where m_0 is the mass of coke before the reaction (g) and m_1 is the mass of coke after the coupling reaction (g).

$$\mathrm{CTS} = \frac{m_2}{m_1} \times 100\% \tag{10}$$

where m_2 is the mass of gasified coke with a size larger than 10 mm after the drum test (g).

$$\mathrm{RI}_t(\%) = \left(\frac{0.111W_1}{0.430W_2} + \frac{M_0 - M_t}{M_0 \times 0.430W_2} \times 100\right) \times 100 \tag{11}$$

where M_0 is the mass of sintering ore before reduction (g), M_t is the mass of sintering ore after t min of experiment (g), and W_1 and W_2 are the FeO and TFe content of sintering ore before experiment, respectively (%).

4. RESULTS AND DISCUSSION

4.1. Gasification of Typical Coke and Reduction of Sintering Ore after Coupling Reaction. Figure 3 shows the relationship between CRE and temperature after the coupling reaction. As shown in Figure 3, when $\varphi(H_2)$ is 25% in a high hygrogen-rich atmosphere, the CRE of both cokes increases with increasing temperature, especially when the temperature is higher than 900 °C, which indicates that the higher the temperature is, the more likely coke gasification occurs and the higher the reactivity of coke is. This is because after H_2 participates in the indirect reduction of sintering ore, a large amount of H_2O will be produced, and H_2O reacts with coke by water-gas reaction, which aggravates the deterioration of coke, which is consistent with the results of the thermodynamic calculation. When the temperature is lower than 900 °C, the change of CRE of the two cokes is not particularly obvious, and it is speculated that this is mainly affected by the thermodynamic conditions of the reaction.

When the reaction temperature is less than 1000 °C, the CRE of L-R coke is slightly higher than that of H-R coke. When the reaction temperature is higher than 1000 °C, the CRE of L-R coke is lower than that of H-R coke. The difference in CRE

https://doi.org/10.1021/acsomega.2c04064
ACS Omega 2022, 7, 34420−34427

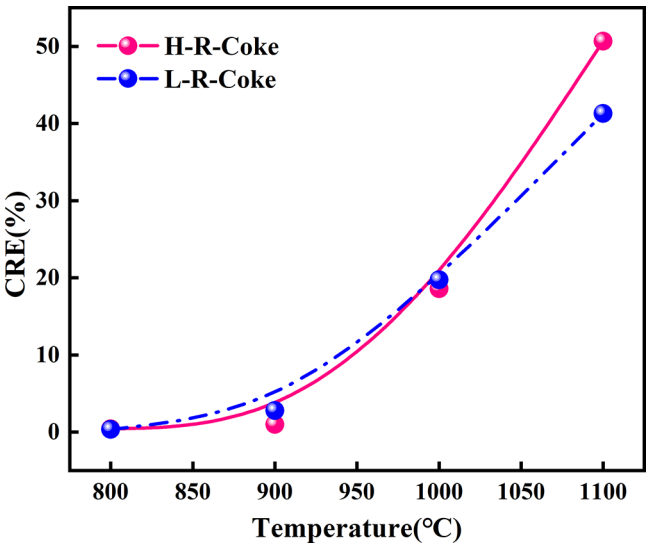

Figure 3. Relationship between CRE and temperature after the coupling reaction.

between L-R coke and H-R coke under a simulated BF atmosphere is not substantial.

Figure 4 shows the relationship between CTS and temperature after the coupling reaction. As shown in Figure 4, with the

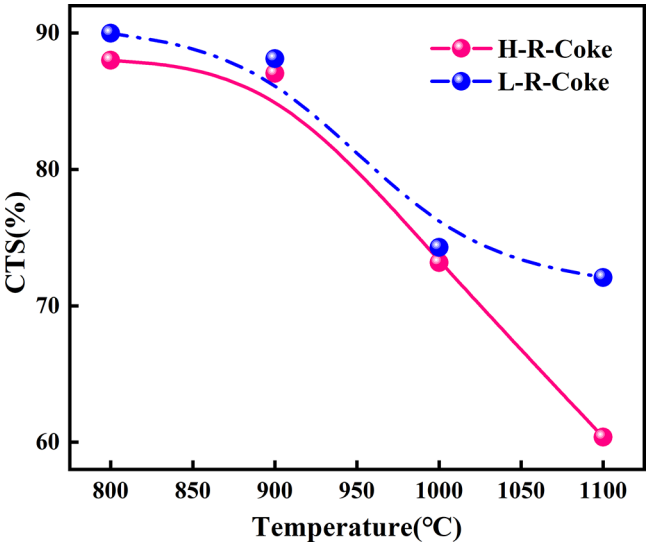

Figure 4. Relationship between CTS and temperature after the coupling reaction.

increase in reaction temperature, the strength of H-R coke and L-R coke after the coupling reaction decreased significantly, and the dissolution loss was considerable, especially when the temperature was higher than 900 °C. The analysis shows that with the increase in reaction temperature, H_2O produced by sintering ore reduction in the lower part of the reaction tube increases, and the water-gas reaction gets triggered at a high temperature. The dissolution loss of coke is affected by H_2O and CO_2, which leads to the decrease of coke strength after hydrogen enrichment. The diagram of the coupling reaction between coke gasification and sinter reduction is shown in Figure 5.

The difference in CRI and CSR between H-R coke and L-R coke was 28.2 and 44.42%, respectively, under the national standard test conditions. The CRE of H-R coke and L-R coke

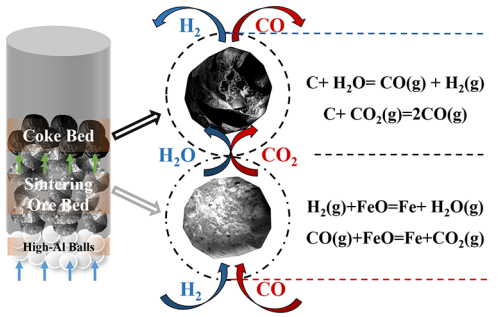

Figure 5. Diagram of coupling reaction between coke gasification and sintering ore reduction.

after the coupling reaction with sintering ore was negatively correlated with CTS under the atmosphere of $\varphi(H_2)$ = 25%. The difference between CRE and CTS of H-R coke and L-R coke was not obvious, especially when the temperature was lower than 1000 °C. Although the CTS of H-R coke is 60.4% at 1100 °C, it still meets the requirements of a BF for metallurgical coke strength.

The results of the national standard experiment are quite different from the experimental results of this paper. The reason may be that the dissolution reaction of coke is only carried out by pure CO_2 under the national standard experimental conditions, and the coupling reaction between iron-bearing raw materials such as sintering ore and coke is ignored, which is inconsistent with the actual conditions of BF production. CO_2 and H_2O produced by indirect reduction of iron-bearing raw materials such as sintering ore with CO and H_2 are the main causes of coke dissolution loss. It can be seen that the reactivity (CRI) obtained under the national standard test conditions and the strength (CSR) after reaction may mislead the evaluation of high-reactivity coke. When the temperature and atmosphere are close to those of the BF, the test of coke reactivity and strength is more reliable.

Figure 6 shows the relationship between RI_t and temperature after the coupling reaction. It can be seen from Figure 6 that it does not change significantly with temperature after the coupling reaction between sintering ore and L-R coke, all

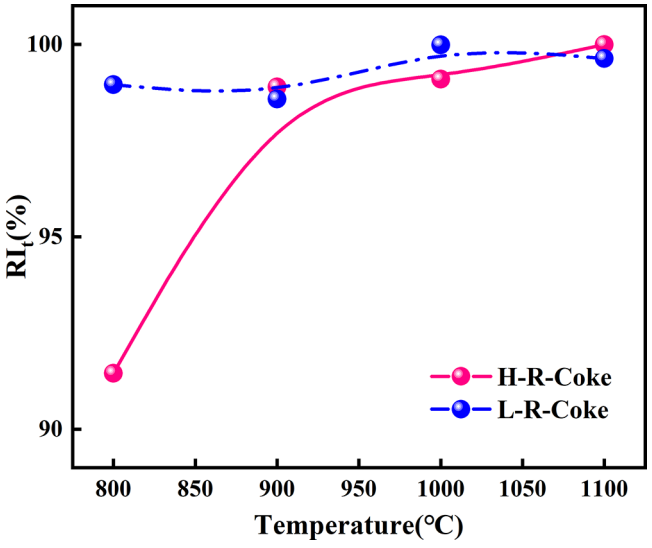

Figure 6. Relationship between RI_t and temperature after the coupling reaction.

https://doi.org/10.1021/acsomega.2c04064
ACS Omega 2022, 7, 34420−34427

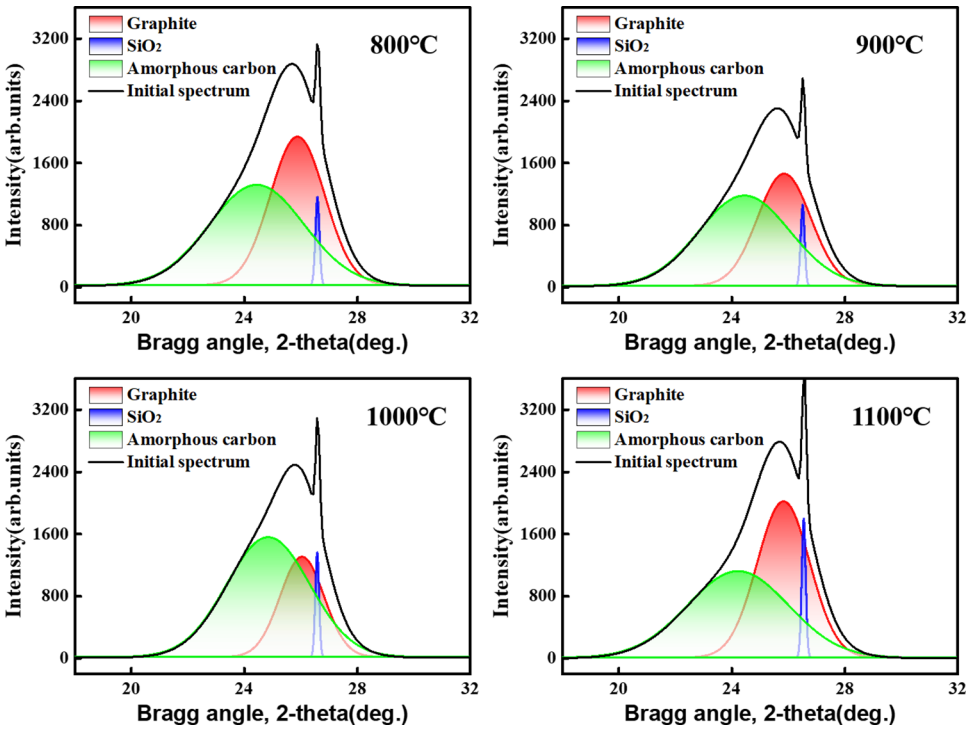

Figure 7. XRD patterns of L-R coke under the influence of temperature.

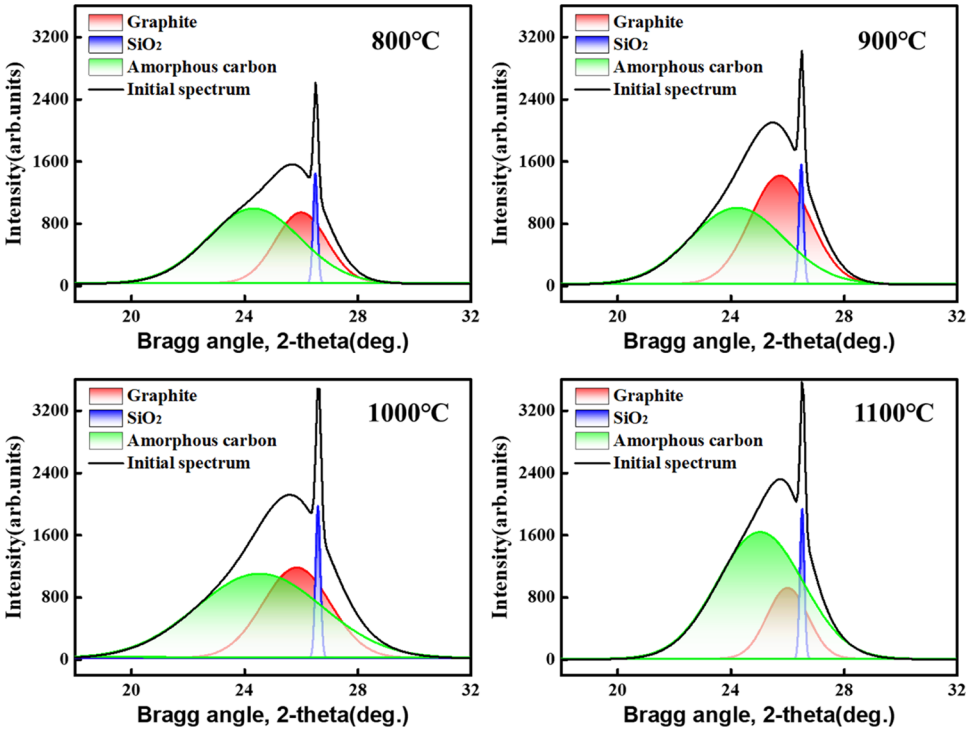

Figure 8. XRD patterns of H-R coke under the influence of temperature.

above 98%. When the temperature is lower than 900 °C, the RI_t of the coupling reaction between H-R coke and sintering ore is lower than that of L-R coke, but when the temperature is higher than 900 °C, the difference between them is not obvious. The reason is that the reaction rate (CRE) of H-R coke gradually increases with the increase of temperature, that is, the reduction gases CO and H_2 produced by the gasification reaction of H-R coke with CO_2 and H_2O increase, thus improving the reduction of sintering ore. Therefore, the coupling effect of H-R coke and sintering ore promotes the reduction of sinter. This is similar to the research results of Kashihara et al.[24] Through experiments and mathematical model analysis, they found that the reduction rate of ore and the gasification rate of coke in the mixed layer of ore and coke were accelerated due to the mutual utilization of the gases produced by the reaction.

https://doi.org/10.1021/acsomega.2c04064
ACS Omega 2022, 7, 34420−34427

4.2. Effect of Temperature on the Carbon Structure of Coke. The peak fitting method was used to distinguish the peaks with the diffraction angle of 18−32° in the XRD spectrum. After peak fitting, XRD spectra were deconvolved into the peaks of graphite, SiO_2, and amorphous carbon. The XRD spectra of the 002 carbon peaks of L-R coke and H-R coke after reactions at 800, 900, 1000, and 1100 °C are shown in Figures 7 and 8, respectively. It can be seen from Figure 7 that the graphitization degree of L-R coke decreases first and then increases, and it is the lowest at 1000 °C. The width of the 002 carbon peak of L-R coke first widened and then narrowed with the increase of temperature, which was the widest at 1000 °C, indicating that the order of the carbon structure of L-R coke first decreased and then increased with the increase of temperature.

Figure 8 shows that when the temperature is 800 and 1000 °C, the 002 carbon peak of H-R coke is wide and diffuse, indicating that the order of the carbon structure is poor. In addition, the width of the 002 carbon peak of L-R coke is narrower than that of H-R coke, indicating that the carbon structure of L-R coke is more orderly than that of H-R coke. The relative content of SiO_2 in H-R coke is higher than that in L-R coke.

The carbon structure and pore characteristics of metallurgical coke have a significant impact on coke behavior and reactivity in a blast furnace. The basic unit of the carbon structure is a graphite crystallite, and the size of the graphite crystallite can usually be characterized by the stacking height *Lc* of the carbon substrate.[25,26] In this study, the stacking height *Lc* was calculated using Origin. First, the XRD data was drawn, and then the "multipeak fitting" was carried out. The Lorentz function was used to obtain the corresponding peak position 2θ and FWHM, and then the stacking height *Lc* was calculated by the Scherrer equation.

$$Lc = \frac{0.8\lambda}{B\cos\theta} \tag{12}$$

where λ is the wavelength of the X-ray radiation, nm; B is the full width at half-maximum of the 002 peak, deg; and θ is the Bragg angle of the 002 peak, deg.

Figure 9 shows the relationship between the stacking height *Lc* of two cokes with different reactivities and temperatures. It is found from Figure 9 that in the range of 800−1100 °C, the *Lc* value of L-R coke decreases first and then increases with the increase in temperature. The *Lc* value of H-R coke is higher at 900 and 1100 °C but lower at 800 and 1000 °C. In addition, the *Lc* value of H-R coke is lower than that of L-R coke, which indicates that the graphitization degree and carbon structure order of L-R coke are higher than those of H-R coke. According to the change of CRE of the two kinds of coke after coupling reaction, it was found that when the reaction temperature was 800−1000 °C, the graphitization degree of coke was positively correlated with its reaction activity. When the reaction temperature was higher than 1000 °C, the graphitization degree of coke was negatively correlated with its reaction activity.

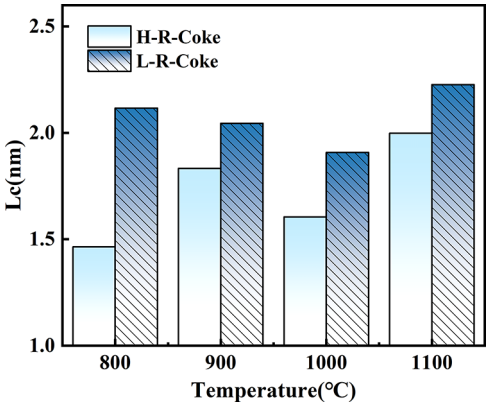

Figure 9. Relationship between the stacking height *Lc* of coke and temperature.

4.3. Effect of Temperature on the Pore Structure of Coke. The pore structure of coke is characterized by the pore wall area, pore wall thickness, and pore size. It is an important reaction interface in the gasification process of coke in a BF and determines the kinetic conditions of the coke gasification process. When $\varphi(H_2)$ is 25% in a high hydrogen-rich atmosphere, the effects of temperature on the pore structure of H-R coke and L-R coke are shown in Figures 10 and 11,

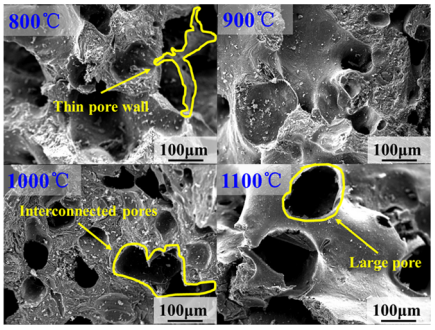

Figure 10. SEM photographs of H-R coke after coupling reaction.

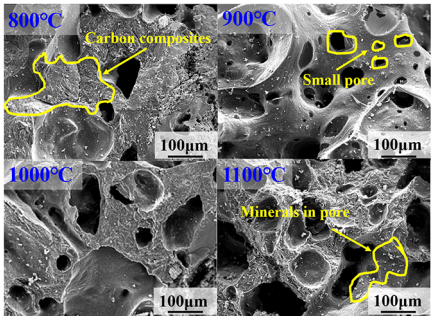

Figure 11. SEM photographs of L-R coke after coupling reaction.

respectively. For H-R coke, when compared with the pore structure at 800 and 900 °C, the number of pores at 1000 and 1100 °C is greater, and even a large number of perforations are produced. At the same time, the size of pores becomes larger, and the thickness of the pore wall decreases significantly, thereby increasing the reaction interface of CO_2 and H_2O with coke gasification reaction, resulting in more serious damage to the carbon matrix of coke. This indicates that the higher the temperature, the more serious the dissolution loss of coke, thus affecting the thermal strength of metallurgical coke.

The changing trend of the pore structure of L-R coke with temperature is basically consistent with that of H-R coke. However, comparing the microstructure of different cokes under the same experimental conditions, it can be seen that the pore structure formed by high-reactivity coke is larger, and the pore size of low-reactivity coke is smaller. Notably, although the microstructure of blast furnace coke may control its reactivity and strength to some extent, it is not the only criterion. The multiphase reaction in a BF, alkali metal, and the composition of

https://doi.org/10.1021/acsomega.2c04064
ACS Omega 2022, 7, 34420−34427

coke itself also directly affect the dissolution loss behavior of metallurgical coke.

5. CONCLUSIONS

The coupling behavior between gasification of typical coke and reduction of sintering ore in a $CO-N_2-H_2$ gas mixture with $\varphi(H_2)$ of 25% at different temperatures was studied using a conventional coke reactivity measuring device. The following conclusions were reached:

(1) According to the thermodynamic calculation results, when the temperature is lower than 1100 K, with the increase of $\varphi(H_2)$ in the initial reaction gas, the concentration of reducing gas in the system increases when the reduction reaction of iron oxide reaches equilibrium, and the gasification of coke is inhibited. When the temperature is higher than 1100 K, the results are the opposite.

(2) The CRE of both cokes increased with the increase in temperature, and CTS decreased with the increase in temperature. The CTS of L-R coke after the reaction is higher than that of H-R coke, and the RI_t of sintering ore after the coupling reaction with L-R coke is higher than that with H-R coke.

(3) At a high temperature and high hydrogen-rich atmosphere with $\varphi(H_2)$ of 25%, the CTS of H-R coke is greater than 60.4%, which meets the strength requirements of a blast furnace for metallurgical coke. It can be seen that the reactivity (CRI) obtained under the national standard test conditions and the strength (CSR) after reaction may mislead the evaluation of high-reactivity coke.

(4) The graphitization degree and carbon structure order of L-R coke are higher than those of H-R coke. When the reaction temperature is 800−1000 °C, the graphitization degree of coke is positively correlated with its reactivity, and when the reaction temperature is greater than 1000 °C, it is negatively correlated.

AUTHOR INFORMATION

Corresponding Author

Yuelin Qin − *School of Metallurgy and Materials Engineering, Chongqing University of Science and Technology, Chongqing 401331, China; Value-Added Process and Clean Extraction of Complex Metal Mineral Resources, Chongqing Municipal Key Laboratory of Institutions of Higher Education, Chongqing 401331, China*; Phone: +86-185-2392-5702; Email: qinyuelin@cqust.edu.cn

Authors

Jinglan Hu − *School of Metallurgy and Materials Engineering, Chongqing University of Science and Technology, Chongqing 401331, China*; orcid.org/0000-0002-3010-6346

Xin Li − *School of Metallurgy and Materials Engineering, Chongqing University of Science and Technology, Chongqing 401331, China*

Haowen Liu − *School of Metallurgy and Materials Engineering, Chongqing University of Science and Technology, Chongqing 401331, China*

Yin Deng − *School of Metallurgy and Materials Engineering, Chongqing University of Science and Technology, Chongqing 401331, China*

Hao Liu − *School of Metallurgy and Materials Engineering, Chongqing University of Science and Technology, Chongqing 401331, China; Value-Added Process and Clean Extraction of Complex Metal Mineral Resources, Chongqing Municipal Key Laboratory of Institutions of Higher Education, Chongqing 401331, China*

Complete contact information is available at: https://pubs.acs.org/10.1021/acsomega.2c04064

Notes

The authors declare no competing financial interest.

ACKNOWLEDGMENTS

This research was funded by the National Natural Science Foundation of China (Nos. 51974054 and 52174300) and Natural Sciences Foundation of Chongqing, China (No. cstc2021ycjh-bgzxm0211).

REFERENCES

(1) Mousa, E. A.; Babich, A.; Senk, D. Enhancement of iron ore sinter reducibility through coke oven gas injection into the modern blast furnace. *ISIJ Int.* **2013**, *53*, 1372−1380.

(2) Higuchi, K.; Matsuzaki, S.; Saito, K.; Nomura, S. Improvement in reduction behavior of sintered ores in a blast furnace through injection of reformed coke oven gas. *ISIJ Int.* **2020**, *60*, 2218−2227.

(3) Guo, T. L.; Chu, M. S.; Liu, Z. G.; Wang, Z. C.; Tang, J.; Fu, X. J. Exergy analysis on blast furnace with coke oven gas injection. *J. Cent. South Univ.* **2013**, *44*, 3108−3114.

(4) Guo, T. L.; Liu, Z. G.; Chu, M. S. Numerical simulation of blast furnace raceway with coke oven gas injection. *J. Northeast Univ.* **2012**, *33*, 987−991.

(5) Silaen, A. K.; Okosun, T.; Chen, Y.; Wu, B.; Zhou, C. Q. Investigation of high rate natural gas injection through various lance designs in a blast furnace. *Iron Steel Technol.* **2015**, *1*, 1536−1549.

(6) Guo, T. L.; Chu, M. S.; Liu, Z. G.; Tang, J.; Junichiro, Y. Mathematical modeling and exergy analysis of blast furnace operation with natural gas injection. *Steel Res. Int.* **2013**, *84*, 333−343.

(7) Liu, X.; Qin, X.; Chen, L.; Sun, F. CO_2 emission optimization for a blast furnace considering plastic injection. *Int. J. Energy Environ.* **2015**, *6*, 175−190.

(8) Murai, R.; Asanuma, M.; Sato, M.; Inoguchi, T.; Terada, K. Flow behavior of plastic particles in the lower part of blast furnace. *ISIJ Int.* **2015**, *55*, 528−535.

(9) Wang, P.; Zhang, Y. Q.; Long, H. M.; Wei, R. F.; Li, J. X.; Meng, Q. M.; Yu, S. C. Degradation behavior of coke reacting with H_2O and CO_2 at high temperature. *ISIJ Int.* **2017**, *57*, 643−648.

(10) Wang, P.; Yu, S.; Long, H.; Wei, R.; Meng, Q.; Zhang, Y. Microscopic study on the interior and exterior reactions of coke with CO_2 and H_2O. *Ironmak. Steelmak.* **2017**, *44*, 595−600.

(11) Wang, P.; Zhang, Y. Q.; Li, J. X.; Long, H. M.; Meng, Q. M.; Yu, S. C. Effects of CO_2 and H_2O on solution loss reaction of coke. *Chin. J. Process Eng.* **2016**, *16*, 138−143.

(12) Chang, Z. Y.; Wang, P.; Zhang, J. L.; Jiao, K. X.; Zhang, Y. Q.; Liu, Z. J. Effect of CO_2 and H_2O on gasification dissolution and deep reaction of coke. *Int. J. Miner. Metall. Mater.* **2018**, *25*, 1402−1411.

(13) Zhang, H. Gasification of metallurgical coke in CO_2-CO-N_2 with and without H_2. *Chem. Eng. J.* **2018**, *347*, 440−446.

(14) Xu, R.; Dai, B.; Wang, W.; Schenk, J.; Bhattacharyya, A.; Xue, Z. Gasification reactivity and structure evolution of metallurgical coke under H_2O/CO_2 atmosphere. *Energy Fuels* **2018**, *32*, 1188−1195.

(15) Lan, C.; Lyu, Q.; Liu, X.; Jiang, M.; Qie, Y.; Zhang, S. Thermodynamic and kinetic behaviors of coke gasification in N_2-CO-CO_2-H_2-H_2O. *Int. J. Hydrogen Energy* **2018**, *43*, 19405−19413.

(16) Wang, W.; Dai, B.; Xu, R.; Schenk, J.; Wang, J.; Xue, Z. The effect of H_2O on the reactivity and microstructure of metallurgical coke. *Steel Res. Int.* **2017**, *88*, No. 1700063.

(17) Guo, W.; Xue, Q.; Liu, Y.; Guo, Z.; She, X.; Wang, J.; Zhao, Q.; An, X. Kinetic analysis of gasification reaction of coke with CO_2 or H_2O. *Int. J. Hydrogen Energy* **2015**, *40*, 13306−13313.

(18) Naito, M.; Okamoto, A.; Yamaguchi, K.; Yamaguchi, T.; Inoue, Y. Improvement of blast furnace reaction efficiency by use of high reactivity coke. *Tetsu-to-Hagane* **2001**, *87*, 357−364.
(19) Nomura, S.; Higuchi, K.; Kunitomo, K.; Naito, M. Reaction behavior of formed iron coke and its effect on decreasing thermal reserve zone temperature in blast furnace. *ISIJ Int.* **2010**, *50*, 1388−1395.
(20) Natsui, T.; Nakano, K.; Matsukura, Y.; Sunahara, K.; Ujisawa, Y.; Inada, T. Evaluation of sinter reducibility and coke reactivity by experimental blast furnace. *Tetsu-to-Hagane* **2013**, *99*, 267−274.
(21) Wu, S. L.; Tuo, B. Y.; Zhang, L. H.; Guo, L.; Zhou, Y. Influence of coke reactivity on the ferric burden reduction of the lumpy zone in a blast furnace. *Chin. J. Eng.* **2013**, *35*, 282−287.
(22) Wu, S.; Sun, Y.; Kou, M.; Shen, W. Calculation model of using appropriate high reactivity coke in blast furnace. *Steel Res. Int.* **2014**, *85*, 918−926.
(23) Lan, C. C.; Zhang, S. H.; Liu, X. J.; Liu, R.; Lyu, Q. Gasification behaviors of coke in a blast furnace with and without H_2. *ISIJ Int.* **2021**, *61*, 158−166.
(24) Kashihara, Y.; Iwai, Y.; Fukada, K.; Nogami, H. Effect of coke particle arrangement on reduction and gasification reaction in mixed layer of ore and coke. *ISIJ Int.* **2019**, *59*, 1198−1204.
(25) Li, H.; Zhang, H.; Li, K.; Zhang, J.; Sun, M.; Su, B. Catalytic graphitization of coke carbon by iron: Understanding the evolution of carbon Structure, morphology and lattice fringes. *Fuel* **2020**, *279*, No. 118531.
(26) Wang, M.; Liu, Z.; Chu, M.; Shi, Q.; Tang, J.; Han, D.; Cao, L. Influence of temperature and CO_2 on high-temperature behavior and microstructure of metallurgical coke. *ACS Omega* **2021**, *6*, 19569−19577.

NOTE ADDED AFTER ASAP PUBLICATION

This paper was published ASAP on September 15, 2022, with incorrect graphics for Table of Contents, Abstract, and Figure 11. The corrected version was reposted on September 27, 2022.

https://doi.org/10.1021/acsomega.2c04064
ACS Omega 2022, 7, 34420−34427